Microstructural evolutions and stability of gradient nano-grained copper under tensile tests and subsequent storage

2015 IOP Conf. Ser.: Mater. Sci. Eng. 89 012001

(http://iopscience.iop.org/1757-899X/89/1/012001)

Microstructural evolutions and stability of gradient nano-grained copper under tensile tests and subsequent storage

W Chen[1], Z S You[1,2], N R Tao[1] and L Lu[1]

[1] Shenyang National Laboratory for Materials Science, Institute of Metal Research, Chinese Academy of Sciences, 72 Wenhua Road, Shenyang 110016, People's Republic of China
[2] Herbert Gleiter Institute of Nanoscience, Nanjing University of Science and Technology, 200 Xiaolingwei Street, Nanjing 210094, People's Republic of China

E-mail: llu@imr.ac.cn

Abstract. A gradient nano-grained (GNG) surface layer is produced on a bulk coarse-grained Cu by means of a surface mechanical grinding treatment. Homogeneous grain coarsening induced by mechanical deformation is observed in the GNG Cu layer under tensile tests at both 300 K and 123 K. The concurrent grain coarsening during tensile deformation is proven to be also thermally activated, because the extent of grain coarsening of the GNG Cu layer is less significant at 123 K than at 300 K, although a higher flow stress is achieved at 123 K. During the subsequent storage at 258 K after tensile tests, no obvious change can be found for the grain size in the GNG Cu layer deformed at 300 K. In contrast, widespread abnormal grain coarsening is frequently observed in the GNG Cu layer deformed at 123 K and stored for 100 days, which may be caused by the higher stored energy in the non-equilibrium grain boundary structures.

1. Introduction

Nano-grained (NG) metals with grain sizes smaller than 100 nm are generally unstable. Their grains could grow rapidly either under thermal [1] or mechanical loads [2,3]. The former is called thermally-induced grain coarsening relating to the thermal stability of the NG structures whereas the latter is referred to as mechanically-induced grain coarsening associated with the mechanical stability and imposed plastic deformation. Both the thermally- and mechanically-induced grain coarsening are of intimate relevance to the presence of a large volume fraction of grain boundaries (GBs), which possess considerable excess free energy and thus may provide a large driving force for the inherent structural instability.

In regards to the thermal stability of NG metals, there have been many literature reports, but the data seem to be inconsistent. For instance, nano-grains in pure Cu [1] grow even at room temperature (RT) (~0.2 T_m, where T_m is the absolute melting temperature), whereas NG Ni is relatively stable up to 473 K (~0.3 T_m) [4]. Indeed, a large number of NG metals exhibit remarkable thermal stability [5], manifested by a relatively high onset temperature (sometimes as high as 0.6 T_m) of grain coarsening. This unexpected thermal stability of NG metals could be attributed to the kinetic stabilization or thermodynamic stabilization. The kinetic stabilization is achieved by reducing the grain boundary (GB) mobility by solute drag, second-phase particle pinning (Zener pinning), or other mechanism such as porosity drag [5]. The thermodynamic stabilization is achieved by reducing the driving force for grain coarsening through reducing the GB energy via GB segregation [6].

Grain coarsening induced by mechanical deformation at RT has been reported in plenty of NG samples under diverse deformation modes such as indentation [3,7], rolling [8], compression [9] and tensile loading [10]. Specifically, Zhang *et al* [3] reported a significant grain coarsening in NG Cu (10-100 nm) after indentation at both RT and liquid-nitrogen temperature. Even more surprising is the observation that the extent of grain coarsening at liquid-nitrogen temperature is much greater than that at RT [11,12]. They proposed that such a grain coarsening is a primarily stress-induced and athermal process because the appreciably higher stress would be achieved at cryogenic temperature and conductive to the grain coarsening. Afterwards, Gurao and Suwas [8] reported contradictory results that grain coarsening is observed in NG Ni (~20 nm) during rolling at RT, rather than in a cryo-rolled sample, although a higher flow stress level is achieved in the NG Ni at the lower deformation temperature.

More recently, by means of a surface mechanical grinding treatment (SMGT) [13], a spatial gradient nano-grained (GNG) layer was produced on the surface of a bulk coarse-grained (CG) Cu rod. The surface NG layer exhibits a 10 times higher yield strength and a uniform tensile plasticity comparable to that of the CG substrate. The sustained tensile true strain could be as high as 100%, and had not induced any cracking or delamination in the GNG layer, which is starkly different from the behavior observed in free-standing NG metals [14]. The authors pointed out that the plastic deformation of the GNG structure is dominated by mechanically-induced GB migrations which concomitantly cause substantial grain coarsening [15].

For a better understanding of the mechanism of mechanically-induced grain coarsening of GNG Cu, in this study, the mechanical stability including the microstructural evolutions and grain coarsening of GNG Cu was systematically investigated under tensile tests at different temperatures (300 K and 123 K). The investigation was also undertaken with specific objective of studying the thermal stability of GNG Cu after tensile tests, i.e., the effect of the so-called "storage annealing" on the microstructure of GNG Cu during the subsequent storage at 258 K, i.e., −15 ºC, for different numbers of days. Both the mechanisms related to the mechanical stability and thermal stability of the GNG Cu layer will be discussed.

2. Experimental

2.1. Sample fabrication

Commercial-purity copper rods (99.97 wt.%) consisting of well-annealed equiaxed coarse grains (with an average diameter of 25 μm) were machined into dog-bone tensile samples with a gauge length of 20 mm and a gauge diameter of 6 mm. Then both the gauge section and the arc transitions of the samples were subjected to SMGT. The basic principle and detailed procedure of the SMGT process have been described elsewhere [13]. In this study, the applied SMGT processing parameters are as follows: rotation speed υ_1 = 600 rpm, sliding velocity of the tool tip υ_2 = 3 mm s^{-1}, penetration depth of the tool tip into the sample a_p = 40 μm, and the Cu rod was cooled to a cryogenic temperature of ~173 K with liquid nitrogen during the SMGT process. In order to effectively refine the grains in the surface layer and increase the thickness of the nanostructured layer, the SMGT process was repeated six times with the same parameters.

2.2. Tensile tests

Uniaxial tensile tests of the SMGT-processed samples (hereafter referred to as the GNG/CG Cu) were performed on an Instron 5982 testing machine (Instron, UK) with a constant strain rate of 1×10^{-2} s^{-1} at 300 K and 123 K, respectively. The tensile tests at 123 K were carried out in an Instron environment chamber, which was cooled by liquid-nitrogen flow. An Instron 2620-601 clip-on extensometer was used to measure strain at RT, while an Epsilon model 3542 clip-on extensometer was used to measure strain at 123 K.

Several GNG/CG Cu samples were stretched to two predefined true strains of ε_T = 4% (shortly after the yield point) and 23% (well-developed in the uniform plastic deformation stage) and then unloaded for further microstructural examination at both temperatures. All the samples before and after tensile deformation were refrigerated at 258 K. To avoid the possibility of spontaneous grain coarsening in the GNG Cu layer during the storage, all the examinations including mechanical tests and microstructural characterising of the samples were finished within 5 days, unless otherwise specified.

2.3. Microstructural characterization

In order to reveal the microstructural evolutions, the longitudinal sections of the as-treated and tensile strained GNG/CG Cu samples were examined by a FEI NanoSEM Nova 430 scanning electron microscope (SEM) and by a JEOL-2010 transmission electron microscope (TEM) operated at a voltage of 200 kV. To protect the surface NG layer, a pure Cu layer was electro-deposited onto the surface. Then longitudinal samples were cut by using an electric spark cutting machine (ESM). Samples for SEM observation were polished first mechanically and then electrochemically in a solution of phosphoric acid (25%), alcohol (25%), and deionized water (50%) at RT. Samples for TEM observation were first mechanically polished to a final thickness of ~40 μm, then thinned by twin-jet polishing in an electrolyte of 33% phosphoric acid and 67% deionized water (by volume) at about −10 ºC.

The grain size distributions of the top GNG Cu surface layer at different conditions were determined on bright-field TEM images. Over 800 grain sizes were measured from about 60 TEM images for each data set.

3. Results

3.1. Microstructure of the as-SMGT (GNG/CG) samples

The longitudinal cross-sectional SEM image in figure 1a shows a typical hierarchical microstructure of as-SMGT Cu samples, which apparently varies with the depth along the radial direction. This spatial microstructural gradient is formed by the SMGT technique that simultaneously imposes a high strain rate and a strong strain gradient at the sample surface. After the treatment, the surface is very flat and shining with a minor roughness ($R_a \approx 0.3$ μm), and crack-free.

Closer observations by TEM indicate that the top 20 μm thick surface layer is completely composed of nano-sized grains with an average grain size of 50 nm (the average transversal and longitudinal axis grain sizes are 42 nm and 60 nm, respectively) as shown in figure 1b. The selected-area electron diffraction (SAED) pattern (inset of figure 1b) indicates that the nano-grains are randomly oriented. The majority of the nano-sized grains are separated by indistinct curved or wavy GBs, which are apparently in a non-equilibrium state, as generally observed in nanostructured metals refined by severe plastic deformation [16]. These deformation distorted GBs are characterized by the presence of a high-density of extrinsic GB dislocations and hence of relatively high stress concentrations around GBs.

The average grain size gradually increases to about 350 nm as the depth increases from 20 to 100 μm (figures 1c and d). The grains are still nearly equiaxed. Beneath 100 μm, a typical deformation structure can be observed, which is characterized by dislocation tangles and dislocation cells with a size also gradually increasing from submicrometres to micrometres with the depth. The thickness of the overall deformed surface layer is about 700 μm. Therefore, the spatial gradient structure introduced by SMGT consists of a GNG layer, a deformed CG layer and an undeformed CG core. In this study, since only the evolution of NG structure is concerned, particular attention is paid to the top GNG layer (20 μm thick) with grain sizes smaller than 100 nm.

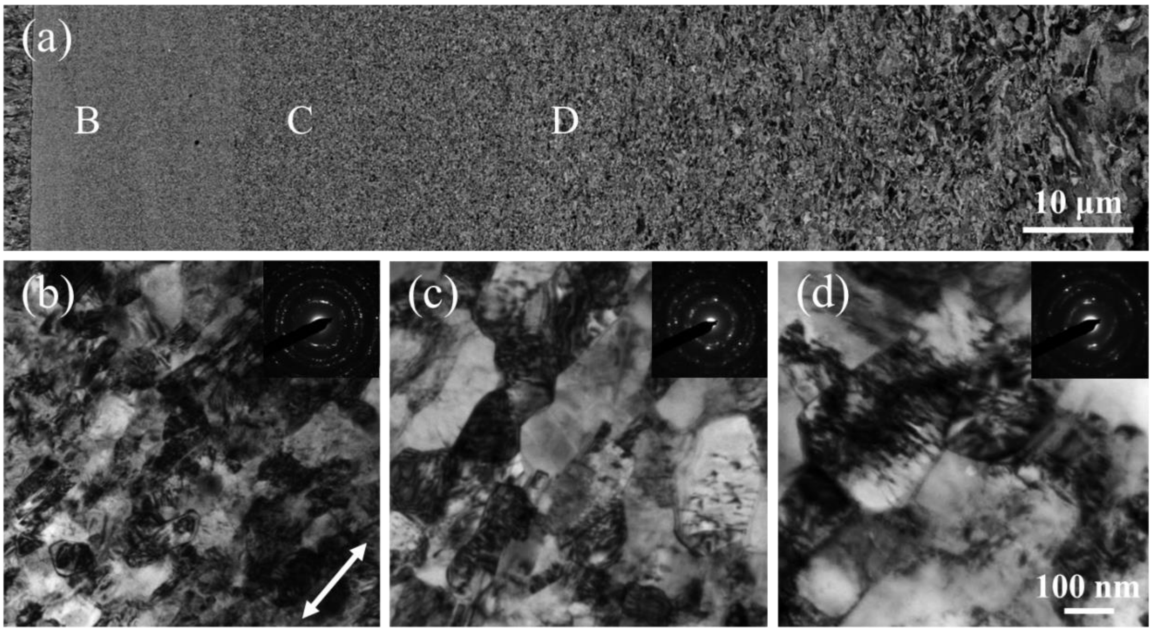

Figure 1 (a) Typical longitudinal section SEM image of a SMGT Cu sample. (b, c and d) Bright-filed TEM images at positions B, C and D indicated in (a), respectively. The double-head arrow indicates the tensile loading direction (the same as in the following Figures).

3.2. Microstructural evolutions of GNG Cu layer during tensile deformation

Tensile tests indicated that the GNG/CG Cu exhibits an obvious temperature dependence of the yield strength (0.2% offset). When the temperature decreases from 300 to 123 K, the yield strength of GNG/CG Cu elevates from 129 to 149 MPa, while a negligible enhancement of yield strength is observed in CG Cu. The relative stronger temperature dependence of the yield strength of the GNG/CG Cu sample suggests that the GNG Cu layer sustains a much higher tensile stress at 123 K than at 300 K. This is consistent with the literature report that the hardness of NG Cu with a grain size of 11 nm increased from 2.1 to 4 GPa, as the temperature decreased from 300 to 123 K [17].

Postmortem TEM observations (figures 2a-d) on samples tensioned to different strains under diverse temperatures provide an insight into the microstructural evolutions of the GNG Cu. Compared with the as-SMGT state (figure 1b), homogeneous grain coarsening is observed in the top GNG Cu layer after tensile deformation at 300 K (figures 2a and b). Moreover, the dislocation density in the microstructure is also greatly reduced, as indicated by the more uniform image contrast in the grains. As the strain increases from ε_T = 4% (figure 2a) to 23% (figure 2b) at 300 K, grains in the GNG Cu layer become larger in size and elongated slightly (the aspect ratio at ε_T = 23% is 1.9). Accompanying the grain coarsening, most of the GBs become straighter and sharper, which implies a more equilibrium state.

Homogeneous grain coarsening is also detected in the GNG Cu layer after tensile deformation at 123 K (figures 2c and d), although the extent of grain coarsening is less significant than that at 300 K. Furthermore, a high density of dislocations is retained in the microstructure due to the suppressed recovery at the lower deformation temperature. As the strain increases from ε_T = 4% (figure 2c) to 23% (figure 2d), grains in the top GNG Cu layer become larger but still remain equiaxed (the aspect ratio at ε_T = 23% is 1.5). Most of the GBs in the GNG Cu layer deformed at 123 K are indistinct and curved, indicating that they are still in a non-equilibrium state.

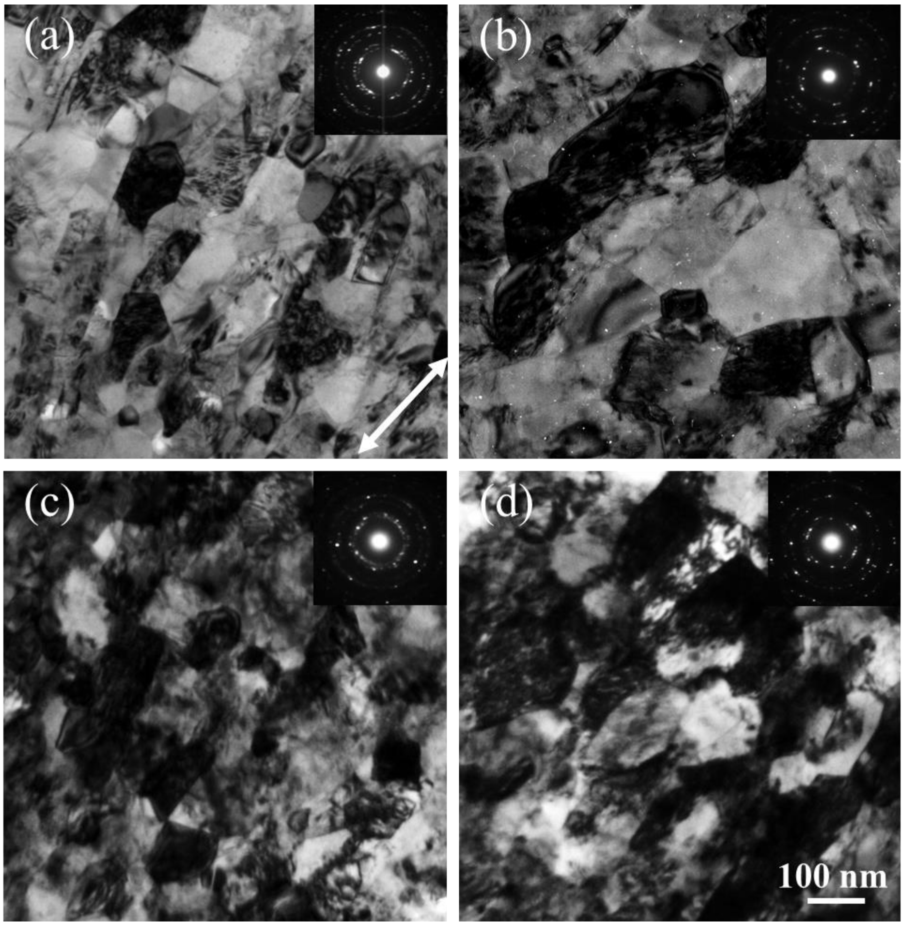

Figure 2 Bright-field TEM images showing the typical microstructures of the top GNG surface layer (2.5 μm below the sample surface) at different tensile temperatures and different strains. (a) ε_T = 4%, 300 K. (b) ε_T = 23%, 300 K. (c) ε_T = 4%, 123 K. (d) ε_T = 23%, 123 K.

Grain coarsening during tensile deformation is described more quantitatively in the form of transversal grain size distribution plots of the grain area fraction versus grain size at various temperatures and strains (figures 3a-d). The transversal grain size distribution of the as-SMGT sample is quite narrow ranging from 20 to 80 nm. With increasing tensile strains to ε_T = 4% and 23%, the transversal grain size distributions become broader at both 300 K (figures 3a and b) and 123 K (figures 3c and d). Moreover, the small grains in the GNG layer have gradually disappeared. It is noted that the transversal grain size distributions at 123 K (figures 3c and d) are much narrower and concentrating at the small grain size regime compared with that at 300 K (figures 3a and b), which indicates a less significant grain coarsening at 123 K. Examination of the longitudinal grain size distributions also gives the same but more obvious evidence that the extent of grain coarsening of the GNG Cu layer is less significant at 123 K (figures 4c and d) than that at 300 K (figures 4a and b). Furthermore, the unimodal grain size distributions at different temperatures and different strains also confirm that the grain coarsening accompanying tensile deformation is in a uniform mode.

It is interesting to find that although the GNG Cu layer sustains a much higher mechanical stress at 123 K than that at 300 K, the extent of grain coarsening induced by tensile deformation is less significant at 123 K. This suggests that the mechanical stability of the GNG Cu layer increases as the deformation temperature decreases.

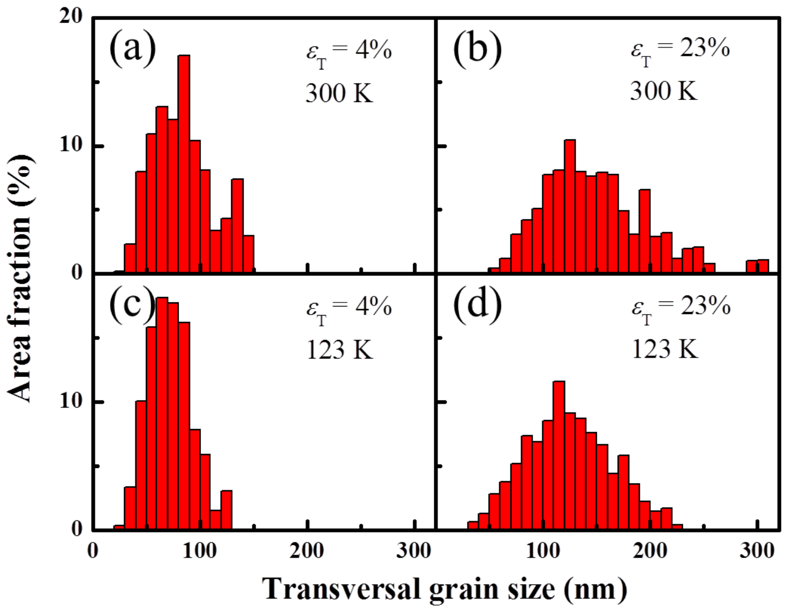

Figure 3 Area-weighted transversal grain size distributions in the top GNG surface layer at different temperatures and strains, as indicated.

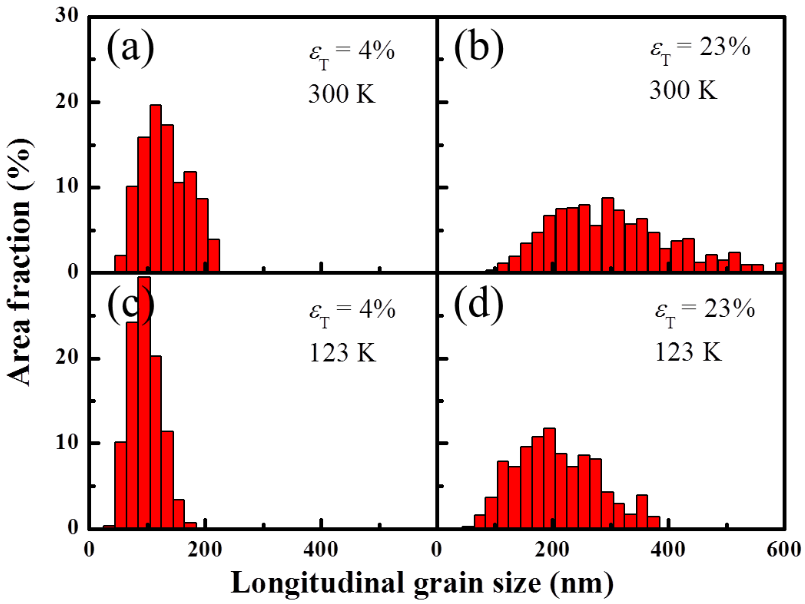

Figure 4 Area-weighted longitudinal grain size distributions in the top GNG surface layer at different temperatures and strains, as indicated.

3.3. Microstructural evolution of GNG Cu during storage at 258 K

After tensile tests, the GNG Cu samples deformed to ε_T = 23% at different temperatures were further stored at 258 K for different numbers of days. No obvious change in grain size can be found in the GNG Cu deformed at 300 K with increasing storage time under the resolution of the SEM observations (figures 5a-c). TEM images show more details for the microstructures of the GNG Cu layer with ε_T = 23% and stored for 10 days (figure 6a) and 30 days (figure 6b). Compared with the microstructure of the GNG Cu layer just after tension (figure 2b), no obvious change can be found in the microstructure during the storage (figures 6a and b), except for a slight decrease in the dislocation density.

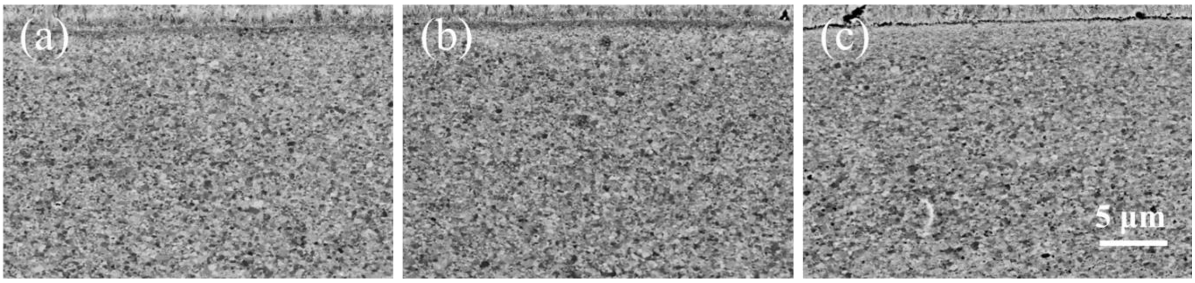

Figure 5 SEM images of the top GNG Cu layers with ε_T = 23% deformed at 300 K and stored at 258 K for 10 days (a), 30 days (b) and 100 days (c), respectively.

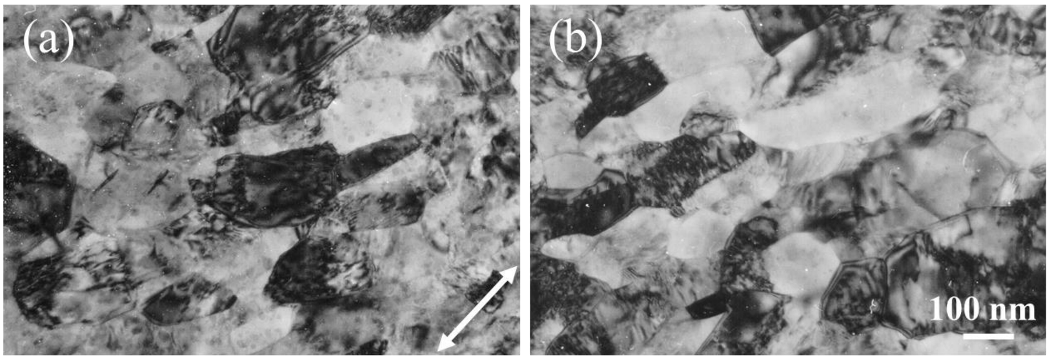

Figure 6 TEM images showing the typical microstructures of the top GNG Cu layers with ε_T = 23% deformed at 300 K and stored at 258 K for 10 days (a) and 30 days (b). No significant difference between the microstructures can be detected.

In contrast to the stable microstructure of the GNG Cu deformed at 300 K and stored at 258 K, the storage of the 123 K deformed GNG Cu at 258 K leads to the formation of very large grains in the matrix of fine grains, as clearly shown in the SEM observations (figure 7b for 30 days, and figure 7c for 100 days). These abnormally large grains are formed during the storage rather than in the tensile deformation processes, because only homogeneously distributed small grains in the GNG Cu are detected just after being stored for a short period of 3.5 hours (figure 7a). Moreover, it is worth noting that the abnormal grain coarsening is not an accident, but a common phenomenon. For example, widespread abnormally large grains with a grain size larger than a few micrometres are frequently observed in the GNG Cu layer stored for 100 days as shown in figure 7d.

To make sure whether the grain size is stable in the areas apart from the abnormally large grains as indicated by the square in figure 7b, closer TEM observations were applied to examine the fine grain areas in the GNG Cu layer deformed at 123 K and stored for 30 days. Obviously, even in the small grain size areas, abnormal grain coarsening had also occurred (figure 8a). It is noted that the dislocation density in the large grain (with a longitudinal grain size of 800 nm) is rather low, which is in sharp contrast to the high density of dislocations in the surrounding small grains. The GBs of the large grains are also much sharper than that of the small ones, which means a more equilibrium state. It is interesting to find that some clean and straight twin boundaries can be observed in some large grains (with a grain size usually larger than 1 μm) as shown in figure 8b, although the sample is stored at low temperatures.

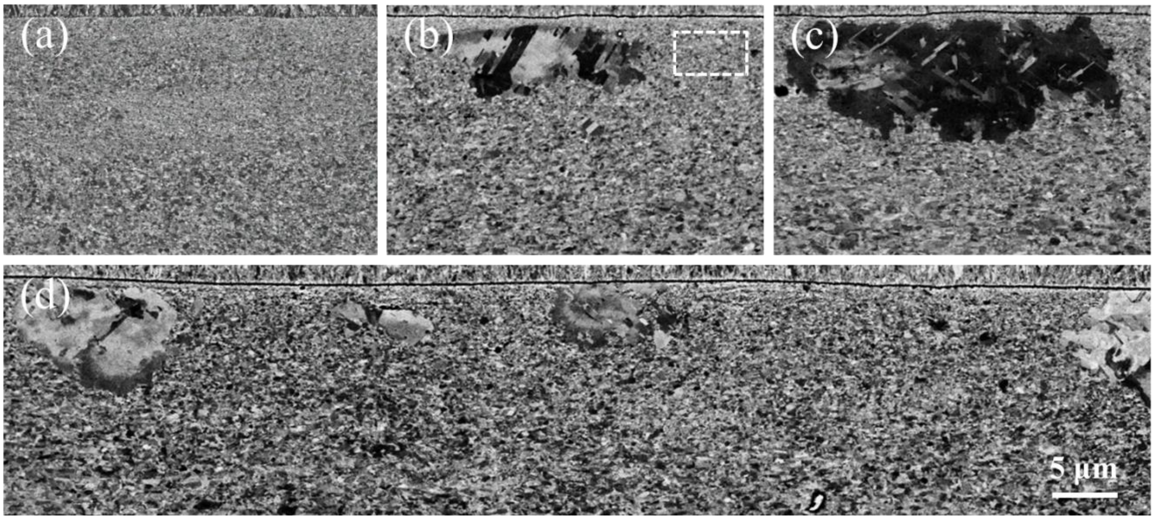

Figure 7 SEM images of the top GNG Cu layers which were deformed to ε_T = 23% at 123 K and stored at 258 K for 3.5 hours (a), 30 days (b) and 100 days (c), respectively. (d) An SEM picture with a large field of view of the sample stored for 100 days displays the widespread abnormal grain coarsening.

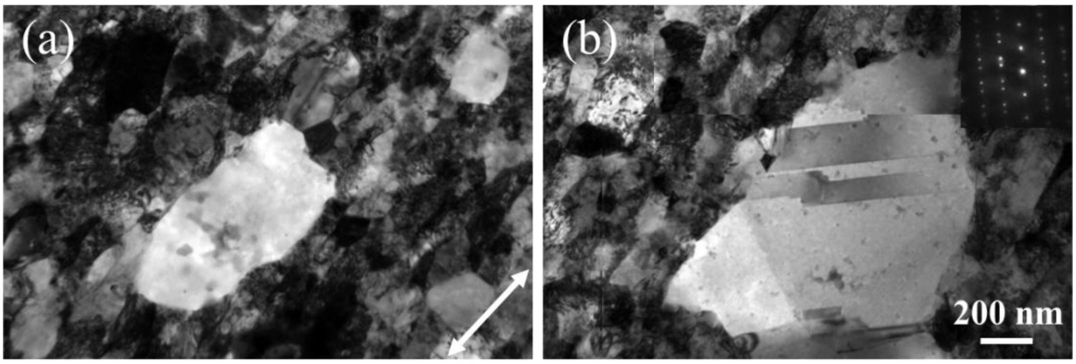

Figure 8 TEM images showing the relative small grain size areas of the GNG Cu layers deformed to ε_T = 23% at 123 K and subsequently stored at 258 K for 30 days. (a) A large dislocation-free grain is found to be embedded in the small grains. (b) An abnormally large grain is divided by clear (1 1 1) twin boundaries as indicated by the SAED patterns.

4. Discussion

Deformation-induced GB migration and associated grain coarsening have been experimentally verified to dominate the plastic deformation of various NG systems [10,15,18]. However, the understanding of detailed underlying mechanism is still far from mature. Computer molecular dynamics simulations have also been performed aiming at atomistically revealing the GB migration behavior [19-21], but the ultra-high strain rate and limited available time scale inevitably rule out some processes which may operate under realistic laboratory conditions. On the other hand, the grain coarsening mechanism can also be indirectly investigated by experimentally exploring the influence of such parameters as deformation temperature [3,8,22], strain rate [23,24], stress state [2,25] on the degree of grain growth, or by scrutinizing the character and evolution of the microstructure, especially the GB structure.

In this study, the grain coarsening behavior of the GNG Cu layer is investigated by tensile tests at different temperatures (300 K and 123 K) to reveal the temperature effect. The microstructural observations reveal a quite homogeneous normal grain coarsening accompanying tensile deformation at both temperatures, as shown in figures 2. Furthermore, the extent of grain coarsening increases with increasing tensile strain. However, at a given plastic strain, the grains grow less significantly when the sample is deformed at 123 K than at 300 K, indicating that reducing temperature appears to suppress the deformation-induced grain coarsening. Taking account of the fact that the surface GNG Cu layer sustains a higher flow stress at low temperatures, this result is clearly an indication that the grain coarsening during the deformation of NG structures is not exclusively controlled by the stress.

Zhang *et al* [3,11,12] reported that the grain coarsening in NG Cu under indentation at liquid-nitrogen temperature is more significant than at RT, suggesting that the athermal stress-induced GB migration and grain growth mediates the plastic deformation. The contrary in the temperature effect on the grain coarsening between the present result and the literature may be associated with the difference in the stress or strain state of the samples under mechanical deformation. Below the indentation, a larger strain gradient and complex stress state may change the dominant process controlling grain coarsening by facilitating the stress-induced GB migration. However, in the GNG Cu layer supported by a CG core that suppresses its strain localization, the nano-grains deform homogeneously under uniaxial tensile stresses. Although the detailed process of the mechanically-induced grain coarsening in the GNG Cu is still not well understood, it is reasonable to speculate that in order to accommodate the homogeneous grain growth, some GB activities other than the athermal stress-induced GB migration must also be triggered together. The more significant grain coarsening of the GNG Cu at higher deformation temperatures (RT versus 123 K) irrespective of being under lower applied stresses is a thermally activated process.

In addition to the extent of grain coarsening, the deformation temperature also exerts a strong influence on the deformation microstructure of the GNG Cu layer. It is noted that the GBs in the 300 K tensioned GNG Cu are in a much more equilibrium state, and appear straight and sharp, in stark contrast to the as-SMGT state where the GBs occupied by high-density extrinsic dislocations are indistinct. This suggests that mechanically-induced GB migration in GNG Cu deformed at RT has consumed the accumulated dislocations nearby, leading the GBs to a low energy state. By contrast, in the 123 K deformed GNG Cu, most GBs are still curved and blurred, in a non-equilibrium state. Inside the grains, there are a high-density of dislocations and strong stress contrast. The diverse GB states for GNG Cu deformed at 300 K and 123 K probably reflect different thermally activated grain coarsening behavior, and can also rationalize the thermal stability of deformed samples as discussed below.

The excess free energy due to GBs can be estimated by the Gibbs-Thomson relationship [26]:

$$\Delta G = \frac{4\Omega\gamma}{d} \tag{1}$$

where Ω is atomic volume, γ is the GB energy and d is the mean diameter of the grains. In the 123 K tensioned GNG Cu, the GBs are in a high-energy state due to the accumulation of high density defects. The energy of such non-equilibrium GBs can be two or more times the equilibrium GB energy [27]. Furthermore, the grain size in the 123 K tensioned GNG Cu is smaller than that in the GNG Cu deformed at 300 K. Thus, according to equation (1) and in view of both the smaller grain size and the higher GB energy, the GNG Cu deformed at 123 K should have higher excess free energy compared to the one deformed at 300 K. During the subsequent storage at 258 K, obvious abnormal grain growth is observed in the GNG Cu layer deformed at 123 K, but not in the GNG Cu layer deformed at 300 K. This suggests that the deformation at 300 K has completely eliminated the defects of and hence reduced the energy of nanoscale GBs in the course of grain coarsening.

It is noted that the grain growth in the GNG Cu deformed at 123 K and stored at 258 K for several tens of days is in an abnormal mode, which is usually observed for the low temperature grain coarsening of the NG metals [28]. The traditional hypothetical factors linked to the occurrence of abnormal grain coarsening such as inhomogeneous purities drag and pores drag seem impossible to apply to our samples. Several other factors may contribute to the abnormal grain growth in this study. Firstly, the stored energy in the GNG Cu layer introduced by plastic deformation may not be homogeneous and will cause nucleation and growth of defect-free grains preferentially at localized areas with the highest stored energy. Secondly, some larger dislocation-free grains induced by the mechanical deformation may directly act as nuclei for the abnormal grain growth.

The present results suggest that the thermal stability of NG metals is strongly dependent on its deformation history. All the factors related to the stored energy, final grain size as well as GB energy or morphology will have a direct impact on the microstructural stability during subsequent annealing treatment or storage.

5. Summary

The microstructural evolutions and mechanical/thermal stability of GNG Cu under tensile tests (at 300 K and 123 K) and subsequent storage at 258 K were systematically investigated by means of SEM and TEM. The GNG Cu layer sustains a higher stress at 123 K but the resulting grain coarsening is less significant compared with that caused by deformation at 300 K. The mechanically-induced grain coarsening can also be thermally activated in the GNG Cu. During subsequent storage at 258 K for tens of days, an obvious abnormal grain coarsening is observed in the GNG Cu layer deformed at 123 K, but not at 300 K under the same storage condition. The lower thermal stability of the sample deformed at 123 K may be caused by the larger stored energy at GBs. The insight into the stabilities of nanostructures gained in this work could be valuable for understanding the microstructural stability of NG metals under service process and thermomechanical treatment.

Acknowledgement

The authors acknowledge financial support from the National Basic Research Program of China (973 Program, 2012CB932202), the National Science Foundation of China (Grant Nos. 51420105001, 51171181, 51371171, 51471172 and 51401211). LL thanks the financial support of the "Hundreds of Talents Project" by the Chinese Academy of Sciences. The authors thank Mr. X. Si for SMGT sample preparation.

References

[1] Gertsman V Y and Birringer R 1994 *Scripta Metall. Mater*. **30** 577
[2] Rupert T J, Gianola D S, Gan Y and Hemker K J 2009 *Science* **326** 1686
[3] Zhang K, Weertman J R and Eastman J A 2004 *Appl. Phys. Lett*. **85** 5197
[4] Thuvander M, Abraham M, Cerezo A and Smith G D W 2001 *Mater. Sci. Technol*. **17** 961
[5] Suryanarayana C and Koch C C 2000 *Hyperfine Interact*. **130** 5
[6] Chookajorn T, Murdoch H A and Schuh C A 2012 *Science* **337** 951
[7] Jin M, Minor A M, Stach E A and Morris J W 2004 *Acta Mater*. **52** 5381
[8] Gurao N P and Suwas S 2009 *Appl. Phys. Lett*. **94** 191902
[9] Pan D, Kuwano S, Fujita T and Chen M W 2007 *Nano Lett*. **7** 2108
[10] Gianola D S, Van Petegem S, Legros M, Brandstetter S, Van Swygenhoven H and Hemker K J 2006 *Acta Mater*. **54** 2253
[11] Zhang K, Weertman J R and Eastman J A 2005 *Appl. Phys. Lett*. **87** 061921
[12] Gai P L, Zhang K and Weertman J 2007 *Scripta Mater*. **56** 25
[13] Li W L, Tao N R and Lu K 2008 *Scripta Mater*. **59** 546
[14] Meyers M A, Mishra A and Benson D J 2006 *Prog. Mater Sci*. **51** 427
[15] Fang T H, Li W L, Tao N R and Lu K 2011 *Science* **331** 1587
[16] Li Y S, Tao N R and Lu K 2008 *Acta Mater*. **56** 230
[17] Huang Z, Gu L Y and Weertman J R 1997 *Scripta Mater*. **37** 1071
[18] Fan G J, Fu L F, Choo H, Liaw P K and Browning N D 2006 *Acta Mater*. **54** 4781

[19] Schiøtz J 2004 *Mater. Sci. Eng.*, A **375** 975
[20] Farkas D, Mohanty S and Monk J 2008 *Mater. Sci. Eng.*, A **493** 33
[21] Monk J and Farkas D 2007 *Phys. Rev.* B **75** 045414
[22] Prasad M and Chokshi A H 2012 *Scripta Mater.* **67** 133
[23] Gianola D S, Warner D H, Molinari J F and Hemker K J 2006 *Scripta Mater.* **55** 649
[24] Bachmaier A, Hafok M and Pippan R 2010 *Mater. Trans.* **51** 8
[25] Brandstetter S, Zhang K, Escuadro A, Weertman J R and Van Swygenhoven H 2008 *Scripta Mater.* **58** 61
[26] Gibbs J W and Bumstead H A 1993 *Thermodynamics* Vol 1 (Longmans, Green and Company)
[27] Nazarov A A, Romanov A E and Valiev R Z 1993 *Acta Metall. Mater.* **41** 1033
[28] Ames M, Markmann J, Karos R, Michels A, Tschope A and Birringer R 2008 *Acta Mater.* **56** 4255